Analysis of global bifurcations in a market share attraction model

Gian Italo Bischi[a], Laura Gardini[b], Michael Kopel[c],*

[a]*Istituto di Scienze Economiche,University of Urbino, 61029 Urbino, Italy*
[b]*Istituto di Matematica "E. Levi", University of Parma, Italy and Istituto di Scienze Economiche,University of Urbino, 61029 Urbino, Italy*
[c]*Department of Managerial Economics and Industrial Organization, University of Technology, Theresianumgasse 27, 1040 Vienna, Austria*

Abstract

In this paper we demonstrate how the global dynamics of an economic model can be analyzed. In particular, as an application, we consider a market share attraction model widely used in the analysis of interbrand competition in marketing theory. We analyze the local and global dynamic properties of the resulting two-dimensional noninvertible dynamical system in discrete time. The main result of this paper is given by the study of some global bifurcations that change the structure of the attractors and their basins. These bifurcations are investigated by the use of critical curves, a powerful tool for the analysis of the global properties of noninvertible two-dimensional maps. © 2000 Elsevier Science B.V. All rights reserved.

1. Introduction

For many years the dynamics of economic systems have been studied by focusing on stable equilibrium behavior. New results in the theory of nonlinear dynamical systems make us aware, however, that fluctuations over time are quite common and may be due to the nonlinear relationships between the variables of the system and not to exogenous stochastic influences. More recently, this viewpoint has been accepted by economists and operations researchers, management scientists and organization theorists alike (see, e.g., Day, 1994; Hommes, 1991; Kopel 1996a; Parker and Stacey, 1994; Thietart and Forgues, 1995).

The question usually addressed in the economics literature is that of the creation of complex attractors through sequences of *local* bifurcations. The study of the *global* bifurcations that cause qualitative changes of the attractors and their basin of attraction has been rather neglected (for recent work on global phenomena in economic models, see Gardini, 1992,1993; Brock and Hommes, 1997; Bischi et al., 1998). Our work moves a step towards this less explored direction. In this paper we show how the global dynamics of an economic model can be analyzed by the study of some global bifurcations that change the shape of the chaotic attractors and the structure of their basins of attraction, as some parameters of the model are varied. These bifurcations are analyzed by the use of critical curves, a powerful method for the investigation of the global properties of noninvertible two-dimensional maps. To have a particular application at hand we consider an attraction model which is widely used in marketing theory, where marketing efforts for the different brands determine their market shares. This economic model is interesting because of the global properties that have not been yet sufficiently explored. It is also particularly apt for our purpose, namely to introduce some concepts for the analysis of two-dimensional discrete dynamical systems by analogies to the well-known one-dimensional quadratic map.

The paper is organized as follows. In Section 2 we present the market share attraction model with two competing brands, and in Section 3 we give some general properties of the resulting two-dimensional noninvertible map. The existence of a unique nontrivial steady state is proved and the creation of complex attractors around the fixed point is numerically evidenced. The concepts of critical curves and basin boundaries are introduced and applied to our model. The main results are given in Section 4, where we analyze some global bifurcations which cause qualitative changes in the structure of the attractors and of their basins as some parameters are allowed to vary. The bifurcations that change the structure of the basins are characterized as contact bifurcations due to tangencies between the critical curves of the noninvertible map and the basins' boundaries, and those changing the structure of the chaotic sets are characterized as homoclinic bifurcations due to a contact between arcs of

critical curves and the stable manifold of the saddle fixed point. We end the paper with some conclusions in Section 5.

2. An attraction model with interbrand competition

It seems that in marketing theory the results on nonlinear dynamical systems are of particular importance, as marketing variables are governed by nonlinear relationships over time. Research in marketing theory has been focused on the investigation of pulsing advertising strategies (see Simon, 1982; Mahajan and Muller, 1986; Park and Hahn, 1991; Feinberg, 1992), and more recently on the occurrence of cyclic and chaotic fluctuations in marketing models (see Luhta and Virtanen, 1996; Feichtinger et al., 1994; Hibbert and Wilkinson, 1994). It even has been shown that chaotic advertising policies might be optimal (Kopel et al., 1998).

In what follows we will use a market share attraction model which is widely used by both advertising practitioners and model builders. This family of models is based on the assumption that the only determinant of market share is the attraction which customers feel toward each alternative brand available. More formally, the market share s_{it} for brand i ($i = 1, 2, \ldots, n$) in period t is its attraction A_{it} relative to the total attraction of all brands (see Bell et al., 1975):

$$s_{it} = \frac{A_{it}}{\sum_{j=1}^{n} A_{jt}}. \tag{1}$$

In a differential-effects version of the well-known multiplicative competitive interaction model (see Cooper and Nakanishi, 1988), the attraction A_{it} is specified as

$$A_{it} = \exp(\alpha_i) \prod_{k=1}^{K} X_{kit}^{\beta_{ki}}, \tag{2}$$

where X_{kit} denotes the value of the kth explanatory variable for brand i (e.g., distribution, prices, expenditures for advertising), and K is the number of explanatory variables. The parameter α_i is the effectiveness coefficient for firm i's marketing effort, or brand i's constant component of attraction. The parameter β_{ki} denotes brand i's market-response to the kth marketing-mix element. For more flexible specifications of A_{it} which allow, e.g., for temporal distinctiveness of a brand's marketing actions and unusually strong competitive relationships, see Cooper (1988) or Carpenter et al. (1988). It is important to note that a feature of all these formulations is that the logically consistency requirements (i.e. market shares are nonnegative and the sum is equal to one) is automatically fulfilled.

In what follows we consider a two-brand attraction model $(n = 2)$, where there is only one explanatory variable $(K = 1)$, namely advertising effort. For the derivation of the resulting two-dimensional model which we will analyze in subsequent sections, we make two assumptions. First, we assume that the sales revenue R_{it} for a brand i $(i = 1, 2)$ is proportional to its market share,

$$R_{it} = Bs_{it}, \tag{3}$$

where B is the total customer market expenditure (see also Carpenter et al., 1988). Second, the change in marketing effort is proportional to the profit of the previous period, where profits are the difference between sales revenues and (marketing) costs (see Rossiter and Percy, 1987). We assume that brand managers — in order to determine the marketing effort (advertising budget) of the subsequent period — use a decision rule to adjust their advertising efforts adaptively. Denoting the marketing efforts of the two brands in period t with x_t and y_t respectively, the brand managers' decision rules are

$$
\begin{aligned}
x_{t+1} &= x_t + \lambda_1(Bs_{1t} - x_t)x_t, \\
y_{t+1} &= y_t + \lambda_2(Bs_{2t} - y_t)y_t.
\end{aligned}
\tag{4}
$$

Observe that according to (4) the difference in marketing efforts is proportional to the profits. Furthermore, the level of marketing effort of the previous period also effects the degree of response (see Carpenter et al., 1988). The brand managers use the level of marketing effort (advertising budget) of the previous period as an anchor and adjust for the results of the previous period (see also Tversky and Kahneman, 1975; Sterman, 1989a,b; Kopel, 1996a,b for applications of this type of heuristics). The parameters λ_1 and λ_2 denote the "adjustment speeds". Since we will assume that λ_1 and λ_2 are nonnegative, the decision rules we postulate for capturing the managers' decisions are procyclic. Nonpositive values for the adjustment speeds would capture some kind of compensatory mechanism, see Cowling and Cubbin (1971).

Substituting (2) with x_t and y_t as explanatory variables into (1), and the resulting expression for the market shares s_{1t} and s_{2t} into (4), we end up with the following two difference equations:

$$
\begin{aligned}
x_{t+1} &= x_t + \lambda_1\left(B\frac{x_t^{\beta_1}}{x_t^{\beta_1} + ky_t^{\beta_2}} - x_t\right)x_t, \\
y_{t+1} &= y_t + \lambda_2\left(B\frac{ky_t^{\beta_2}}{x_t^{\beta_1} + ky_t^{\beta_2}} - y_t\right)y_t,
\end{aligned}
\tag{5}
$$

where $k := \exp(\alpha_2 - \alpha_1)$.

3. Local and global analysis of the dynamical system

3.1. General properties of the map

The time evolution of the discrete dynamical system (5) is obtained by the iteration of the two-dimensional map

$$
T: \begin{cases} x' = x + \lambda_1 x \left(B \dfrac{x^{\beta_1}}{x^{\beta_1} + k y^{\beta_2}} - x \right), \\[2ex] y' = y + \lambda_2 y \left(B \dfrac{k y^{\beta_2}}{x^{\beta_1} + k y^{\beta_2}} - y \right), \end{cases} \tag{6}
$$

where β_1, β_2, λ_1, λ_2, k and B are real and positive parameters and $'$ denotes the unit-time advancement operator. In what follows we will consider only values of the exponents β_1 and β_2 in the interval $(0, 1)$ since empirical studies show that realistic values are in this range (see, e.g., Bultez and Naert, 1975).

Map (6) is defined for nonnegative values of x and y because of the presence of the real exponents β_1 and β_2. Moreover, the map is not defined in the origin $O = (0, 0)$ since the denominator vanishes in this point. However, we will see that the origin and its preimages[1] play an important role in the description of the global dynamic properties of the model.

Starting from a given initial condition

$$
(x_0, y_0) \in \mathscr{D} = \mathbb{R}_+^2 \setminus (0, 0), \tag{7}
$$

where $\mathbb{R}_+^2 = \{(x, y) \in \mathbb{R}^2 \mid x \geq 0 \text{ and } y \geq 0\}$ denotes the set of nonnegative state variables, the iteration of (6) generates an infinite sequence of states, or a *trajectory*

$$
\{(x_t, y_t) = T^t(x_0, y_0), \ t = 1, 2, \dots\} \tag{8}
$$

provided that (x_0, y_0), as well as all its images $T^t(x_0, y_0)$ of any rank t, belong to the set $\mathscr{D}$. It is important to notice that even if the initial condition (7) belongs to the set $\mathscr{D}$, the iteration of map (6) may produce negative values after a finite number of iterations and, consequently, it may happen that not the complete trajectory is obtained. In the following we shall call a point $(x_0, y_0) \in \mathscr{D}$ a *feasible point* if its full trajectory is bounded and belongs to $\mathscr{D}$. Such a trajectory will be called a *feasible trajectory*.

Since only feasible trajectories of (6) can represent reasonable time evolutions of the economic system modelled by (5), the first important problem to solve is the delimitation of the set of initial conditions that generate feasible trajectories.

---

[1] A preimage of a point $P = (x_p, y_p)$ is a point $P_{-1} = (x, y)$ such that $T(x, y) = P$. A point P may have more than one preimages (or no preimages) which are obtained by solving system (6), with respect to the unknowns x and y, with $x' = x_p$ and $y' = y_p$.

In Section 3.4 we will give an answer to this question, after we carried out a study of the global properties of the map (6).

An important feature of map (6) is that the two coordinate axes are invariant lines, since $T(x,0) = (x',0)$ and $T(0, y) = (0, y')$. The dynamics of (6) along the x-axis are governed by the one-dimensional map $x' = f_1(x)$, where f_1 is the restriction of T to the x-axis, given by

$$f_1(x) = (1 + \lambda_1 B)x - \lambda_1 x^2. \tag{9}$$

Since the situation is symmetric, the dynamics along the y axis are governed by the one-dimensional map $y' = f_2(y)$, where f_2 is obtained from (9) simply by swapping x and y, index 1 and index 2. The maps f_i, $i = 1, 2$, are conjugated to the standard logistic maps $z' = \mu_i z(1 - z)$, $i = 1, 2$, where the parameters μ_i are given by

$$\mu_i = 1 + \lambda_i B, \quad i = 1, 2, \tag{10}$$

the homeomorphisms being given by $x = (1 + \lambda_1 B)z/\lambda_1$ and $(1 + \lambda_2 B)z/\lambda_2$, respectively. Thus, the properties of the trajectories embedded in the invariant axes can be easily deduced from the well-known properties of the standard logistic map (see e.g. Mira, 1987; Devaney, 1989)

$$z' = f(z) = \mu z (1 - z). \tag{11}$$

Since we will often refer to the dynamical behavior of the standard logistic map, we briefly recall some properties of (11) that will be useful in the following. For $\mu \in [2,4]$ every initial condition $z_0 \in (0, 1)$ generates bounded sequences, converging to a unique attractor included in the trapping interval $[c_1, c]$, where $c = \mu/4$ is the maximum value, critical point of rank 1,[2] and $c_1 = f(c) = (\mu^2(4 - \mu))/16$ is the critical point of rank 2, whereas an initial condition out of the interval $[0, 1]$ generates a sequence diverging to $-\infty$. For $\mu \in (1,3)$ the bounded trajectories converge to the fixed point $z^* = (\mu - 1)/\mu$, whereas for $\mu \in (3, 4)$ the attractor can be a cycle of period k or a cyclic chaotic attractor (apart from particular values of μ at which a Cantor set is an attractor in Milnor sense, see Milnor, 1985). A k-cyclic chaotic attractor is formed by a set of k intervals $\{I_1, \ldots, I_k\}$ such that $f(I_j) = I_{j+1}$, for $j = 1, \ldots, k - 1$, and $f(I_k) = I_1$. Such intervals are bounded by the critical point $c = f(c_{-1})$ and some of its images $c_j = f^j(c)$. For example, at $\mu = 3.592572 \ldots$ the logistic map (11) has a 2-cyclic chaotic attractor A formed by two chaotic intervals (see Fig. 1a): $A = [c_1, c_3] \cup [c_2, c]$, where c, c_1, c_2 and c_3 are critical points of rank 1, 2, 3, and 4, respectively. Notice that the chaotic

---

[2] Following the terminology used in Mira (1987), and Mira et al. (1996), we denote by $c_{-1} = \frac{1}{2}$ the point of maximum, critical point of rank-0, and $c_k = f^{k+1}(c_{-1})$ the critical point of rank $k + 1$. The critical point of rank-1 $c_0 = f(c_{-1})$ is also denoted by c.
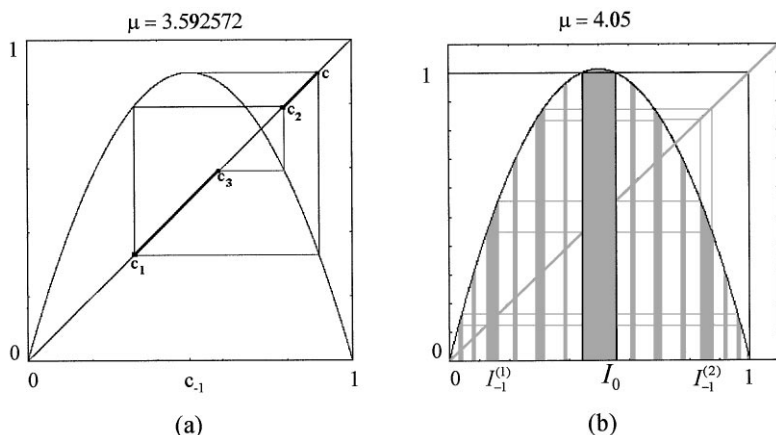
Fig. 1. (a) Standard logistic map with parameter $\mu = 3.592572$. The attractor is given by a 2-cyclic chaotic interval $A = [c_1, c_3] \cup [c_2, c]$, where $c_i = f^{i+1}(c_{-1}) = f^i(c)$ and $c = f(c_{-1})$. The generic traject-ory $\{z_n\}$ starting in $(0, 1)$ enters A after a finite number of iterations, and then never escape from it. (b) Standard logistic map with $\mu > 4$. The points of the interval I_0, as well as those belonging to the infinitely many preimages of any rank of I_0, generate diverging sequences. Only the preimages of I_0 up to rank 2 are represented in the figure.

attractor A, as any attractor of the logistic map for $\mu \in (2, 4)$, is included in the absorbing interval $[c_1, c]$.[3]

For $\mu = 4$ the image c_1 of the critical point c is mapped by (11) into the repelling fixed point in $z = 0$. This represents the *final bifurcation*, after which a generic initial condition $z_0 \in \mathbb{R}$ generates a divergent sequence. In fact, for $\mu > 4$, just after the final bifurcation, a neighborhood I_0 of the critical point $c_{-1} = \frac{1}{2}$ exists, bounded by the two preimages of rank-2 of the origin, whose points exit interval $(0, 1)$ after one iteration, thus giving an unbounded sequence. All the preimages of the points of such a 'main hole' I_0 generate diverging sequences. In Fig. 1b two smaller intervals $I_{-1}^{(1)}$ and $I_{-1}^{(2)}$, rank-1 preimages of I_0 (i.e. whose points are mapped into I_0) are represented, located symmetrically with respect to $c_{-1} = \frac{1}{2}$. Their points exit the interval $(0, 1)$ after two iterations of (11). Defined iteratively, infinitely many preimages of I_0 exist in $[0, 1]$, a few of them are shown in Fig. 1b. The union of all these preimages, whose points generate unbounded sequences, is an open set whose closure is $[0, 1]$. Its complement in $[0,1]$ has zero Lebesgue measure and is a Cantor set (see Guckenheimer and Holmes, 1983; Devaney, 1989).

---

[3] An absorbing interval I is called trapping if the trajectories starting from a point in I never leave the interval, and a neighborhood of I exists whose points enter I after a finite number of steps.

3.2. Fixed points

The fixed points of map (6) are the solutions of the system

$$x\left(B\frac{x^{\beta_1}}{x^{\beta_1} + ky^{\beta_2}} - x\right) = 0,$$

$$y\left(B\frac{ky^{\beta_2}}{x^{\beta_1} + ky^{\beta_2}} - y\right) = 0. \tag{12}$$

There are three evident 'boundary solutions':

$$O = (0,0), \quad E_1 = (B,0), \quad E_2 = (0,B), \tag{13}$$

but O is not a fixed point because the map is not defined in it. The fixed points E_1 and E_2 are related to the fixed points of the one-dimensional quadratic maps f_1 and f_2 governing the dynamics restricted to the invariant axes. There is also another fixed point, interior to the positive quadrant $\mathbb{R}_+^2$, given by the solution of the system

$$B\frac{x^{\beta_1}}{x^{\beta_1} + ky^{\beta_2}} - x = 0,$$

$$B\frac{ky^{\beta_2}}{x^{\beta_1} + ky^{\beta_2}} - y = 0.$$

After some algebraic manipulations it is possible to see that one and only one solution exists, determined by the equation

$$F(x) = k^{1/(1-\beta_2)}x^{(1-\beta_1)/(1-\beta_2)} + x - B = 0.$$

In fact, F is a continuous function with $F(0) < 0, F(B) > 0$ and $F'(x) > 0$ for each $x > 0$, hence a unique positive solution exists, $x^* \in (0, B)$, and the corresponding fixed point is

$$E_* = (x^*, B - x^*). \tag{14}$$

A particularly simple solution is obtained in the case $\beta_1 = \beta_2$: $x^* = B/1 + k^{1/(1-\beta_2)}$.

With a given set of parameters B, β_1 and β_2, the positive fixed point E_* is locally asymptotically stable for sufficiently small values of the adjustment speeds λ_1 and λ_2. As usual in dynamic models with adaptive adjustment, the fixed point E_* loses stability as one or both of the adjustment speeds are increased, and more complex attractors are created around the unstable fixed point. These results are obtained through a standard study of the local stability of the positive fixed point, obtained by a numerical solution of the characteristic equation for the localization, in the complex plane, of the eigenvalues of the Jacobian matrix.

Our attention, however, will be mainly focused on the global properties of the map (6), in particular the boundaries of the chaotic attractors and the boundaries of the set of points that generate feasible trajectories, inside of which the basins of the attractors are included. Since, as we will see in the next subsection, map (6) is noninvertible, its global properties can be characterized by the study of its critical sets (see Gumowski and Mira, 1980; Mira et al., 1996; Abraham et al., 1997).

3.3. Critical curves

The fact that the map T is single-valued does not imply the existence and the uniqueness of its inverse T^{-1}. Indeed, for a given (x', y') the rank-1 preimage (or backward iterate) may not exist or may be multivalued. In such cases T is said to be a noninvertible map. Map (6) belongs to this class, because computing the points (x, y) in terms of a given (x', y') in (6), by solving the system

$$x\left(1 + \lambda_1 B \frac{x^{\beta_1}}{x^{\beta_1} + ky^{\beta_2}} - \lambda_1 x\right) = x',$$

$$y\left(1 + \lambda_2 B \frac{ky^{\beta_2}}{x^{\beta_1} + ky^{\beta_2}} - \lambda_2 y\right) = y', \tag{15}$$

we can have no solution or more than one solution.

In fact, if $x' > (1 + \lambda_1 B)^2/4\lambda_1$ or $y' > (1 + \lambda_2 B)^2/4\lambda_2$ then system (15) has no real solution. This can be easily seen, because from the inequality $x^{\beta_1}/(x^{\beta_1} + ky^{\beta_2}) < 1$ it follows that $x(1 + \lambda_1 Bx^{\beta_1}/(x^{\beta_1} + ky^{\beta_2}) - \lambda_1 x) < x(1 + \lambda_1(B - x))$. This is a concave quadratic function with maximum value $(1 + \lambda_1 B)^2/4\lambda_1$. Hence the left-hand side of the first line of (15) is always less than or equal to $(1 + \lambda_1 B)^2/4\lambda_1$. Analogously from $ky^{\beta_2}/(x^{\beta_1} + ky^{\beta_2}) < 1$ it follows that $y(1 + \lambda_2 Bky^{\beta_2}/(x^{\beta_1} + ky^{\beta_2}) - \lambda_2 y) < y(1 + \lambda_2(B - y)) \leq (1 + \lambda_2 B)^2/4\lambda_2$.

On the other hand, if we compute the preimages of the origin, by solving system (15) with $x' = 0$ and $y' = 0$, we obtain: $0^{(1)}_{-1} = ((1 + \lambda_1 B)/\lambda_1, 0)$; $0^{(2)}_{-1} = (0, (1 + \lambda_2 B)/\lambda_2)$ and $0^{(3)}_{-1}$ located at the intersection of the two curves ω_1^{-1} and ω_2^{-1}, which we will introduce later (see Fig. 4b).

As the point (x', y') varies in the plane $\mathbb{R}^2$ the number of solutions of the system (15), i.e., the number of the rank-one preimages of (x', y'), changes. Pairs of real preimages appear or disappear as the point (x', y') crosses the boundary separating regions whose points have a different number of preimages. Such boundaries are generally characterized by the presence of two coincident (merging) preimages. This leads to the definition of the *critical curves*, one of the distinguishing features of noninvertible maps. The critical curve of rank-1, denoted by LC, is defined as the locus of points having two, or more, coincident rank-1 preimages, located on a set called LC_{-1}. LC is the two-dimensional generalization of the notion of critical value (local minimum or maximum value)

of a one-dimensional map, LC_{-1} is the generalization of the notion of critical point (local extremum point). Arcs of LC separate the plane into regions characterized by a different number of real preimages.

To understand the analogy to one-dimensional maps, recall that for the standard logistic map (11) the critical value is $z' = c = \mu/4$ and the critical point is $z = c_{-1} = \frac{1}{2}$. A point $z' < c$ has two preimages, given by $z_1 = \frac{1}{2} - \sqrt{\mu^2 - 4\mu z'}/(2\mu)$ and $z_2 = \frac{1}{2} + \sqrt{\mu^2 - 4\mu z'}/(2\mu)$, and no preimages if $z' > c$. Thus for logistic map (11) the region Z_2 is the set of points below c, the region Z_0 the set of points above c, and the critical value c is the boundary that separates the two regions. Such a point can be defined as the point with two merging preimages $z_1 = z_2 = c_{-1} = \frac{1}{2}$. Clearly, c_{-1} is a point of noninvertibility for f and this implies, being f continuously differentiable, that c_{-1} is the point in which the first derivative vanishes, and c is its image.

Also for the two-dimensional map T the set of critical points of rank 0, denoted by LC_{-1}, is the locus of coincident rank-1 preimages of the points of LC. Hence in any neighborhood of a point of LC_{-1} there are at least two distinct points mapped by T in the same point near LC. This means that the map T is not locally invertible in the points of LC_{-1} and, since the map (6) is continuously differentiable, we have that LC_{-1} belongs to the set of points where the Jacobian of T vanishes, i.e.

$$LC_{-1} \subseteq \{(x', y') \in \mathbb{R}^2 \mid \det DT = 0\}$$

and LC is the rank-1 image of LC_{-1} under T, i.e. $LC = T(LC_{-1})$.

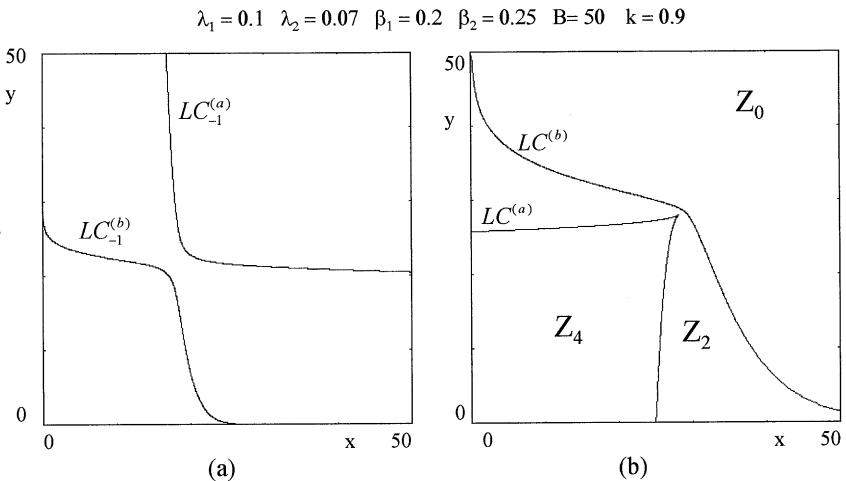$$\lambda_1 = 0.1 \quad \lambda_2 = 0.07 \quad \beta_1 = 0.2 \quad \beta_2 = 0.25 \quad B = 50 \quad k = 0.9$$

Fig. 2. (a) Critical curves of rank-0, obtained as the locus of points such that $\det(DT(x, y)) = 0$. (b) Critical curves of rank-1, obtained as $LC = T(LC_{-1})$. These curves separate the plane into three regions, denoted by Z_4, Z_2 and Z_0 whose points have four, two or no rank-1 preimages respectively.
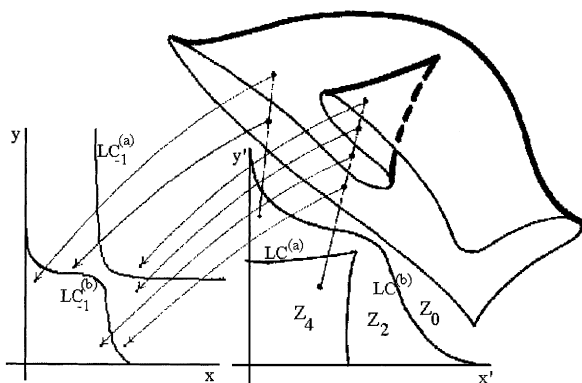
Fig. 3. Riemann foliation for the representation of the inverses of the map T. With each point of the region Z_4 four distinct inverses are associated, each defined on a different sheet of the foliation, whereas points of Z_2 are associated with two sheets. The projection on the phase plane of the folds connecting different sheets are the critical curves LC.

For map (6) the locus of points for which $\det DT = 0$ is given by the union of two branches, denoted by $LC^{(a)}_{-1}$ and $LC^{(b)}_{-1}$ in Fig. 2a. Also LC is the union of two branches, denoted by $LC^{(a)} = T(LC^{(a)}_{-1})$ and $LC^{(b)} = T(LC^{(b)}_{-1})$ (Fig. 2b): $LC^{(b)}$ separates the region Z_0, whose points have no preimages, from the region Z_2, whose points have two distinct rank-1 preimages, and $LC^{(a)}$ separates the region Z_2 from Z_4, whose points have four distinct preimages. In order to study the action of the multivalued inverse relation T^{-1} it is useful to consider a region Z_k of the phase plane as the superposition of k sheets, each associated with a different inverse. Such a representation is known as *Riemann foliation* of the plane (see, e.g., Mira et al., 1996, Chapter 3). Different sheets are connected by folds joining two sheets, and the projections of such folds on the phase plane are arcs of LC. The foliation associated with the map (6) is qualitatively represented in Fig. 3. It can be noticed that the cusp point of LC is characterized by three merging preimages at the junction of two folds.

Note that the branches of critical curves $LC^{(b)}_{-1}$ and $LC^{(b)}$ intersect the coordinate axes x and y in the critical points of rank 0 and 1 of the restrictions f_1 and f_2, given by the points of coordinates

$$c^i_{-1} = \frac{1 + \lambda_i B}{2\lambda_i} \quad \text{and} \quad c^i = f_i(c^i_{-1}) = \frac{(1 + \lambda_i B)^2}{4\lambda_i} \quad i = 1, 2, \tag{16}$$

respectively.

3.4. Boundaries of the feasible set

In the following we denote by $\mathcal{B}$ the *feasible set*, defined as the set of points which generate feasible trajectories. A feasible trajectory may converge to the positive steady state E_*, to other more complex attractors inside $\mathcal{B}$ or to a one-dimensional invariant set embedded inside a coordinate axis (the last occurrence means that one of the two brands disappears). Trajectories starting outside of the set $\mathcal{B}$ represent exploding (or collapsing) evolutions of the economic system. This can be interpreted by saying that the adjustment mechanism expressed by (5) is not suitable to model the time evolution of a system starting outside of the set $\mathcal{B}$.

With values of the parameters β_i in the range $(0.2, 0.3)$, which is a reasonable range according to empirical market investigations (see, e.g., Bultez and Naert, 1975), the invariant coordinate axes appear to be transversely repelling, i.e., they act as repelling sets with respect to trajectories approaching them from the interior of the nonnegative orthant. Moreover, for the parameters used in our simulations, we have observed only one attractor inside $\mathcal{B}$ (although more than one coexisting attractors may exist, each with its own basin of attraction). On the basis of such numerical evidence, in what follows we will often speak of a unique, bounded and positive attracting set, denoted by $\mathcal{A}$, which attracts the generic feasible trajectory, even if its existence and uniqueness are not rigorously proved.

Let $\partial \mathcal{B}$ be the boundary of $\mathcal{B}$. Such a boundary can have a simple shape, as in the situation shown in Fig. 4a, where the attractor $\mathcal{A}$ is the fixed point E_* and $\mathcal{B}$ is represented by the white region, or a very complex structure, as in Fig. 4e, where, again, $\mathcal{B}$ is given by the white points and $\mathcal{A}$ is a chaotic attractor represented by the black points inside $\mathcal{B}$.

An exact determination of $\partial \mathcal{B}$ is the main goal of the remainder of this subsection. Let us first consider the dynamics of T restricted to the invariant axes. From the one-dimensional restriction f_1 defined in (9), conjugated to the logistic map (11), we can deduce that bounded trajectories along the invariant x axis are obtained when $\lambda_1 B \leq 3$ (corresponding to $\mu_1 \leq 4$ in (10)), provided that the initial conditions are taken inside the segment $\omega_1 = OO_{-1}^{(1)}$, where

Fig. 4. In these figures the white regions represent the set $\mathcal{B}$ whose points generate feasible (i.e. positive and bounded) trajectories, the grey ones represent the set of points that generate non-feasible trajectories. (a) The boundary of $\mathcal{B}$ is smooth, and all the feasible trajectories converge to the fixed point E_*. (b) For the same set of parameters as in (a), the segments $\omega_1 = OO_{-1}^{(1)}$ and $\omega_2 = OO_{-1}^{(2)}$ of the invariant axes, and their rank-1 preimages ω_1^{-1} and ω_2^{-1} given by the equations (20) and (21) respectively, are evidenced. (c) For $\lambda_2 > 3/B$ the boundary of $\mathcal{B}$ is fractal. (d) $\mathcal{B}$ is a multiply connected set, due to the presence of *holes* inside it. (e) All the feasible trajectories numerically generated converge to an apparently chaotic attractor.
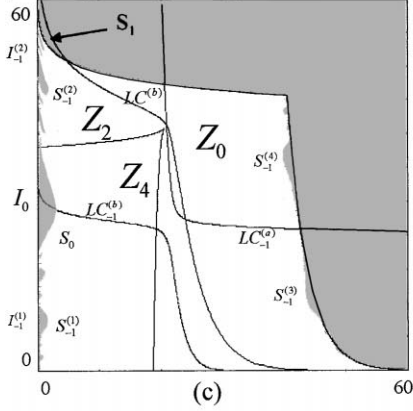
$\lambda_1 = 0.05$ $\lambda_2 = 0.05$ $\beta_1 = 0.2$ $\beta_2 = 0.25$ B= 50 k = 1.2
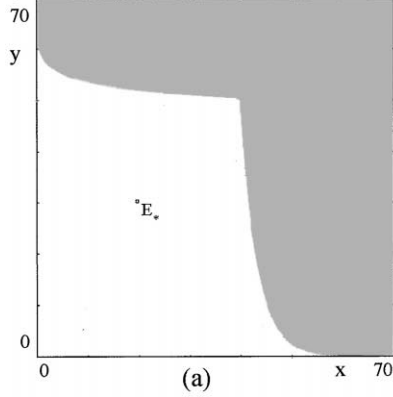
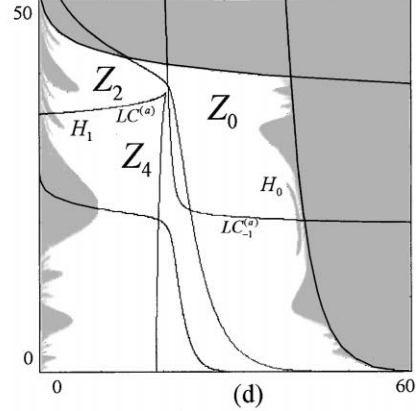$\lambda_1 = 0.05$ $\lambda_2 = 0.05$ $\beta_1 = 0.2$ $\beta_2 = 0.25$ B= 50 k = 1.2
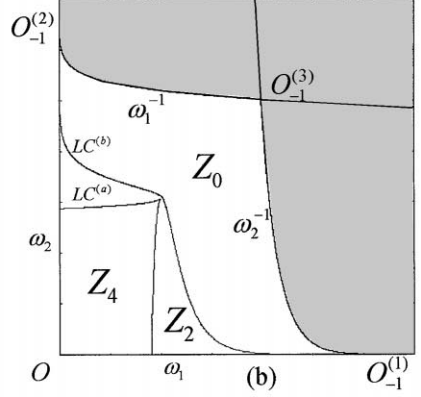
$\lambda_1 = 0.05$ $\lambda_2 = 0.09$ $\beta_1 = 0.2$ $\beta_2 = 0.25$ B= 50 k = 1.2

$\lambda_1 = 0.05$ $\lambda_2 = 0.1$ $\beta_1 = 0.2$ $\beta_2 = 0.25$ B= 50 k = 1.2

$\lambda_1 = 0.05$ $\lambda_2 = 0.1095$ $\beta_1 = 0.2$ $\beta_2 = 0.25$ B= 50 k = 1.2
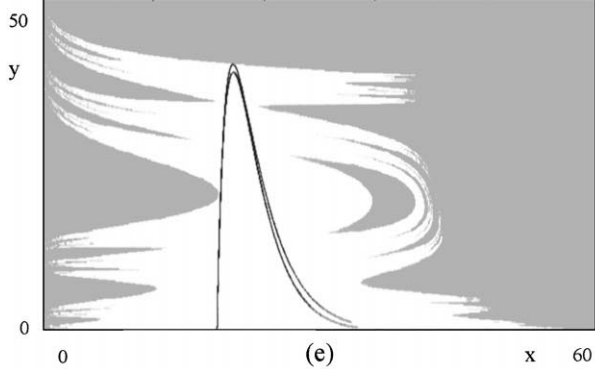
$O^{(1)}_{-1}$ is the rank-1 preimage of the origin O computed according to the restriction f_1 (see Fig. 4b), i.e.

$$O^{(1)}_{-1} = \left(\frac{1 + \lambda_1 B}{\lambda_1}, 0 \right). \tag{17}$$

Divergent trajectories along the x axis are obtained starting from an initial condition out of the segment ω_1. Analogously, when $\lambda_2 B \le 3$, bounded trajectories along the invariant y axis are obtained provided that the initial conditions are taken inside the segment $\omega_2 = 00^{(2)}_{-1}$, where $0^{(2)}_{-1}$ is the rank-1 preimage of the origin computed according to the restriction f_2, i.e.

$$O^{(2)}_{-1} = \left(0, \frac{1 + \lambda_2 B}{\lambda_2} \right). \tag{18}$$

Also in this case, divergent trajectories along the y-axis are obtained starting from an initial condition out of the segment ω_2.

Consider now the region bounded by the segments ω_1 and ω_2 and their rank-1 preimages $\omega_1^{-1} = T^{-1}(\omega_1)$ and $\omega_2^{-1} = T^{-1}(\omega_2)$. Such preimages can be analytically computed as follows. Let $X = (p, 0)$ be a point of ω_1, i.e. $0 < p < (1 + \lambda_1 B)/\lambda_1$. Its preimages are the real solutions of the algebraic system obtained from (6) with $(x', y') = (p, 0)$:

$$x \left(1 + \lambda_1 B \frac{x^{\beta_1}}{x^{\beta_1} + ky^{\beta_2}} - \lambda_1 x \right) = p,$$

$$y \left(1 + \lambda_2 B \frac{ky^{\beta_2}}{x^{\beta_1} + ky^{\beta_2}} - \lambda_2 y \right) = 0. \tag{19}$$

It is easy to see that the preimages of the point X are either located on the same invariant axis $y = 0$ (in the points whose coordinates are the solutions of the equation $f_1(x) = p$) or on the curve of equation

$$x = \left[ky^{\beta_2} \left(\frac{\lambda_2 B - \lambda_2 y + 1}{\lambda_2 y - 1} \right) \right]^{1/\beta_1}. \tag{20}$$

Analogously, the preimages of a point $Y = (0, q)$ of ω_2, i.e. $0 < q < (1 + \lambda_2 B)/\lambda_2$, belong to the same invariant axis $x = 0$, in the points whose coordinates are the solutions of the equation $f_2(y) = q$, or lie on the curve of equation

$$y = \left[\frac{x^{\beta_1}}{k} \left(\frac{\lambda_1 B - \lambda_1 x + 1}{\lambda_1 x - 1} \right) \right]^{1/\beta_2}. \tag{21}$$

It is straightforward to see that curve (20) intersects the y-axis in point $O^{(2)}_{-1}$ given in (18), curve (21) intersects the x-axis in point $O^{(1)}_{-1}$ given in (17), and the two curves (20) and (21) intersect at a point $O^{(3)}_{-1}$ interior to the positive orthant (see

Fig. 4b). As noted before, $O_{-1}^{(3)}$ is another rank-1 preimage of the origin. These preimages of the origin are the vertexes of a 'quadrilateral' $OO_{-1}^{(1)}O_{-1}^{(3)}O_{-1}^{(2)}$, whose sides are ω_1, ω_2 and their rank-1 preimages located on the curves of Eqs. (20) and (21), denoted by ω_1^{-1} and ω_2^{-1} in Fig. 4b. All the points outside this quadrilateral cannot generate feasible trajectories. In fact the points located on the right of ω_2^{-1} are mapped into points with negative x coordinate after one iteration, as can be easily deduced from the first line of (6), and the points located above ω_1^{-1} are mapped into points with negative y coordinate after one iteration, as can be deduced from the second line of (6).

The boundary of $\mathscr{B}$ is given, in general, by the union of all the preimages, of any rank, of the segments ω_1 and ω_2:

$$\partial\mathscr{B}(\infty) = \left(\bigcup_{n=0}^{\infty} T^{-n}(\omega_1)\right) \cup \left(\bigcup_{n=0}^{\infty} T^{-n}(\omega_2)\right). \tag{22}$$

As long as $\lambda_1 B \leq 3$ and $\lambda_2 B \leq 3$ the boundary of $\mathscr{B}$ has the simple shape shown in Fig. 4b. In this situation (obtained with the same parameter values as in Fig. 4a) the quadrilateral $OO_{-1}^{(1)}O_{-1}^{(3)}O_{-1}^{(2)}$ constitutes the whole boundary $\partial\mathscr{B}$, because no preimages of higher rank of ω_1 and ω_2 exist. This is due to the fact that ω_1^{-1} and ω_2^{-1} are entirely included inside the region Z_0 of the plane whose points have no preimages.

The situation is different when the values of the parameters are such that some portions of these curves belong to the regions Z_2 or Z_4 whose points have two or four preimages respectively. In this case preimages of higher order of ω_1 and ω_2 exist, say ω_1^{-k} and ω_2^{-k}, which form new portions of $\partial\mathscr{B}$. Such preimages of ω_1 and ω_2 of rank $k > 1$ bound regions whose points are mapped out of the region $\mathscr{D}$ after k iterations, just as we have shown for the standard logistic map (11) with parameter $\mu > 4$ (see Fig. 1b), i.e. after the contact between the critical point $c = \mu/4$ and the boundary of the basin of infinity at $O_{-1} = 1$. This causes the shape of the boundary of $\mathscr{B}$ to become more complex. In the next section we shall see that, in analogy with the one-dimensional case, also in the two-dimensional case the bifurcations of the basin are characterized by contacts between the basin boundaries and the critical curve LC.

4. Global bifurcations

If λ_1 or λ_2 is increased, so that the bifurcation value $\lambda_b = 3/B$ (which coincides with $\mu = 4$ in (11)) is crossed by at least one of them, then $\partial\mathscr{B}$ is changed from smooth to fractal. This transition between qualitatively different structures of the boundaries of the region $\mathscr{B}$, as some parameters are varied, constitute a *global* (or *non-classical*) *bifurcation* (see Mira et al., 1996). The global

bifurcation occurring at $\lambda_i = \lambda_b$, $i = 1, 2$, can be characterized by a contact between $\partial \mathscr{B}$ and arcs of the critical curves, as described below.

We fix the parameters B, k, β_1, β_2 and λ_1 and vary the speed of adjustment λ_2. As λ_2 is increased, the branch $LC^{(b)}$ of the critical curve that separates Z_0 from Z_2 moves upwards, and at $\lambda_2 = 3/B$ it has a contact with ω_1^{-1} at the point $O^{(2)}_1$. After this contact the sides ω_2 and ω_2^{-1} of $\partial \mathscr{B}$ are transformed from smooth to fractal. In fact, for $\lambda_2 > 3/B$, just after the bifurcation, a segment of ω_1^{-1} enters the region Z_2, so that a portion S_1 of the complement of $\mathscr{B}$, bounded by $LC^{(b)}$ and ω_1^{-1} (see Fig. 4c), now has two preimages. These two preimages, say $S_0^{(1)}$ and $S_0^{(2)}$, merge in points of $LC^{(b)}_1$ (as the points of $LC^{(b)}$ have two merging preimages belonging to $LC^{(b)}_1$) and form a 'gray tongue' issuing from the y axis (denoted by S_0 in Fig. 4c, being $S_0 = S_0^{(1)} \cup S_0^{(2)}$). S_0 belongs to the 'gray set' of points that generate non-feasible trajectories because the points of S_0 are mapped into S_1, so that negative values are obtained after two iterations. The intersection of this 'main tongue' S_0 with the y-axis is given by the neighborhood I_0 of the critical point c^2, defined in (16), of the restriction f_2, i.e. the 'main hole' of the logistic with $\mu > 4$ (see Fig. 1b).

This is only the first of infinitely many preimages of S_1. Preimages of S_1 of higher rank form a sequence of smaller and smaller gray tongues issuing from the y-axis, whose intersection with the y-axis correspond to the infinitely many preimages I_{-k} of the main hole I_0 (see again Fig. 1b). Only some of them are visible in Fig. 4c, but smaller tongues become numerically visible by enlargements, as it usually happens with fractal sets. The fractal structure of the boundary of $\mathscr{B}$ is a consequence of the fact that the tongues are distributed along the segment ω_2 of the y-axis according to the structure of the intervals I_{-k} described at the end of Section 3.1, whose complementary set is a Cantor set.

In the situation shown in Fig. 4c the main tongue S_0 has a wide portion in the region Z_4. Hence, besides the two preimages along the y-axis (denoted by $S_{-1}^{(1)}$ and $S_{-1}^{(2)}$ in Fig. 4c) issuing from the intervals $I_{-1}^{(1)}$ and $I_{-1}^{(2)}$, two more preimages exist (denoted by $S_{-1}^{(3)}$ and $S_{-1}^{(4)}$ in Fig. 4c) issuing from ω_2^{-1} and located at opposite sides with respect to $LC^{(a)}_1$. The tongues $S_{-1}^{(3)}$ and $S_{-1}^{(4)}$ belong to Z_0, hence they do not give rise to new sequences of tongues, whereas $S_{-1}^{(1)}$ and $S_{-1}^{(2)}$ have further preimages, being located inside Z_4 and Z_2 respectively. If the preimages are two, as in the case of $S_{-1}^{(2)}$, they form two tongues issuing from the y-axis, whereas in the case of four preimages, as in the case of $S_{-1}^{(1)}$, two of them are tongues issuing from the y-axis and two are tongues issuing from the opposite side, i.e. ω_2^{-1}.

As λ_2 is further increased, $LC^{(b)}$ moves upwards, the portion S_1 enlarges and, consequently, all its preimages (i.e. the infinitely many tongues) enlarge and become more pronounced. This causes the occurrence of another global bifurcation, that changes the set $\mathscr{B}$ from simply connected to multiply connected (or connected with holes), by a mechanism similar to that described in Mira et al. (1994), Mira et al. (1996, Chapter 5) and Abraham et al. (1997, Chapter 5). This

bifurcation occurs whenever a tongue, belonging to Z_2, has a contact with $LC^{(a)}$ and enters the region Z_4. If the contact occurs out of the y-axis, it causes the creation of a pair of new preimages, merging along $LC^{(a)}_{-1}$, whose union is a *hole* (or *lake*, following the terminology introduced in Mira et al., 1994) inside $\mathscr{B}$, i.e., a set of points that generate non-feasible trajectories surrounded by points of $\mathscr{B}$. This can be seen in Fig. 4d, where the hole H_0 is the preimage of the portion H_1, inside Z_4, of a tongue that crossed $LC^{(a)}$.

As λ_2 is increased, other tongues cross $LC^{(a)}$ and, hence, new holes are created, giving a structure of $\mathscr{B}$ like the one shown in Fig. 4e, where many holes inside $\mathscr{B}$ are clearly visible.

To sum up, the transformation of the set $\mathscr{B}$ from a simply connected region with smooth boundaries into a multiply connected set with fractal boundaries occurs through two types of global bifurcations, both due to contacts between $\partial\mathscr{B}$ and branches of the critical set LC.

As it can be noticed from Figs. 4a and e, also the attractor $\mathscr{A}$ existing inside $\mathscr{B}$ changes its structure for increasing values of the parameter λ_2. For low values of λ_2, as in Fig. 4a, the attractor is the fixed point E_*, to which all the trajectories starting inside the set $\mathscr{B}$ converge. As λ_2 increases, E_* loses stability through a flip (or period doubling) bifurcation at which E_* becomes a saddle point, and an attracting cycle of period 2 is created near it. As λ_2 is further increased, also the cycle of period two undergoes a flip bifurcation at which an attracting cycle of period 4 is created, which becomes the unique attractor inside $\mathscr{B}$. In this case the generic[4] trajectory starting inside $\mathscr{B}$ converges to the 4-cycle, so that $\mathscr{B}$ can be identified with its basin of attraction for any practical purpose. These flip bifurcations are followed by a sequence of period doublings (similar to the well known Myrberg or Feigenbaum cascade for one-dimensional maps), which creates a sequence of attracting cycles of period 2^n followed by the creation of chaotic attractors, which may be cyclic chaotic sets or a connected chaotic set. The numerical simulations show that the size of the chaotic attractor increases as λ_2 increases, and with the parameter values used in Fig. 4e the chaotic set has a contact with the boundary of its basin. This contact bifurcation is known as *final bifurcation* (Mira et al., 1996; Abraham et al., 1997), and causes the destruction of the attractor $\mathscr{A}$. After this contact bifurcation the generic initial strategy generates non-feasible trajectory, that is, the adjustment mechanism (5) does not generate a stable feasible evolution of the economic system.

---

[4] Not all the points of $\mathscr{B}$ generate trajectories converging to the 4-cycle because we must exclude the invariant sets, like the repelling fixed point E_* as well as the points of the repelling 2-cycle whose flip bifurcation generated the attracting 4-cycle, and their stable sets. However, the subset of points in $\mathscr{B}$ which do not converge to the 4-cycle is a set of measure zero, and this justifies the term 'generic'.

Of course, the same sequence of local and global bifurcations occurs if the other speed of adjustment, λ_1, is increased. The only difference is that at the bifurcation value $\lambda_1 = \lambda_b = 3/B$ the contact between $\partial \mathscr{B}$ and LC occurs at the point $O^{(1)}_{-1}$ and consequently the infinitely many tongues with fractal structure are created along the segment ω_1 of the x-axis. Preimages of some of these tongues, those belonging to Z_4, appear along the opposite side ω_1^{-1} of the quadrilateral.

If both the speeds of adjustment λ_1 and λ_2 are greater than the bifurcation value $\lambda_b = 3/B$, tongues appear along all the four sides of the quadrilateral $OO^{(1)}_{-1}O^{(3)}_{-1}O^{(2)}_{-1}$, as it can be seen in the numerical simulations shown in Fig. 5. For the set of parameters used in these figures, the bifurcation value is $\lambda_b = 0.06$, and both λ_1 and λ_2 are always greater than λ_b, so that the boundary of $\mathscr{B}$ has a fractal shape. It can be noticed that the tongues appearing along the x-axis are more pronounced than those appearing along the y-axis. This is due to the fact that $k < 1$, i.e. the relation $\alpha_1 > \alpha_2$ holds between the constant components of attraction. The opposite effect occurs if $k > 1$.

In Figs. 5 we show different types of attractors that can be obtained by varying the parameters λ_i and β_i. In Fig. 5a the attractor $\mathscr{A}$ inside the set $\mathscr{B}$ is a cycle of period 4, represented by the four small dots. As both the speeds of adjustment are increased, a sequence of period-doubling bifurcations gives rise to cycles of period 2^k and then to cyclic chaotic attractors, like the 2-cyclic chaotic attractor shown in Fig. 5b. In this situation the long-run behavior of the system is characterized by cyclical behavior of order two, but in each period the exact state cannot be predicted. If the speeds of adjustment λ_i are further increased, the two-piece chaotic area has a contact with $\partial \mathscr{B}$ (in Fig. 5c we are just before such a bifurcation) and then it disappears being this the final bifurcation. With a different change in the parameters, for example by using slightly lower values of the parameters β_i the two-cyclic chaotic attractor gives rise to a connected chaotic attractor, as in Fig. 5d, after a contact of the two chaotic areas. This is due to the first homoclinic bifurcation of the saddle fixed point E_*, as we shall see in greater detail below, and this leads to a further loss of information about the long-run behavior of the system: a cyclic (although chaotic) behavior is replaced by a totally erratic evolution that covers a wide area of the phase space of the dynamic system.

Critical curves are also quite helpful in the analysis of the boundaries of the chaotic attractors. In fact, in analogy to the critical points of the one-dimensional maps, that together with their images determine the boundaries of the chaotic intervals (as recalled at the end of Section 3.1, see Fig. 1a) the critical curve LC and its images can be used to bound invariant absorbing areas, which include the two-dimensional chaotic attractors of noninvertible maps. In two-dimensional maps the notion of chaotic area generalizes that of chaotic intervals, and the critical curves, that constitute the generalization of the concept of critical points, are expected to play a similar role in determining the boundaries
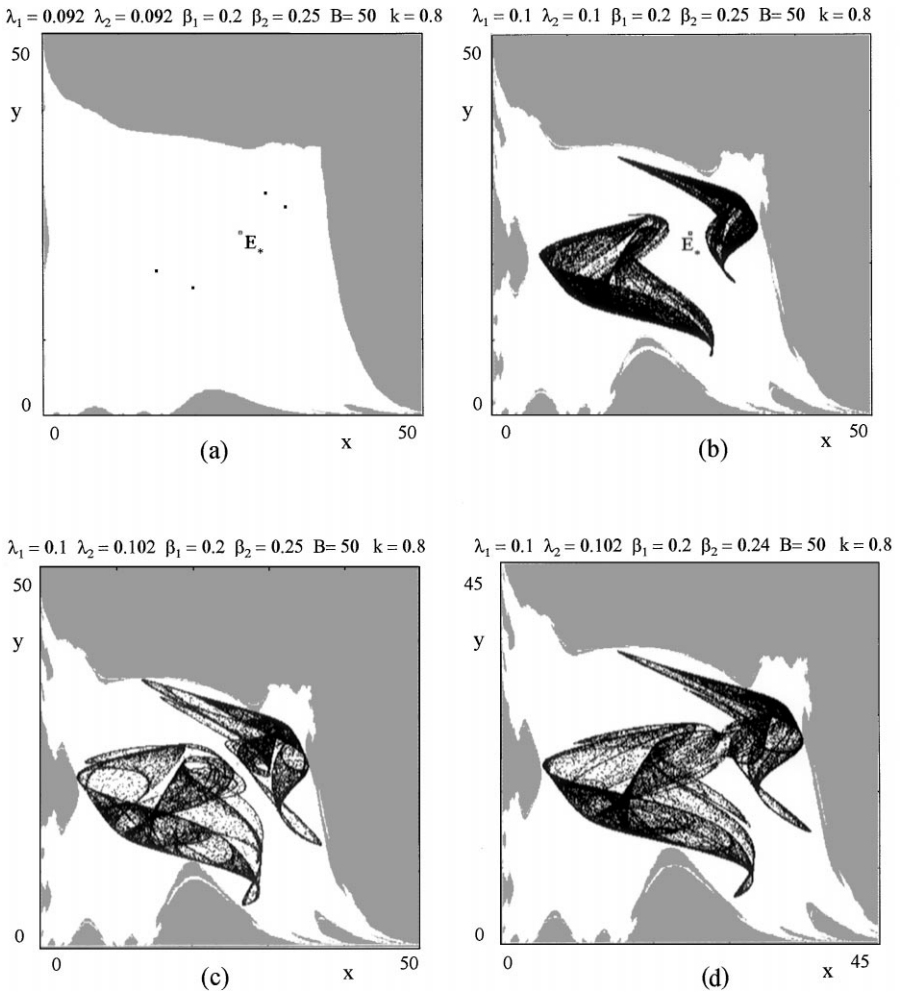
Fig. 5. Some attractors to which the generic feasible trajectory converges.

of the chaotic areas (see Mira et al., 1996, for a definition of the concept of chaotic area and for the proofs that critical arcs bound such areas). We recall that the critical sets of rank k are the images of rank k of LC_{-1} denoted by $LC_{k-1} = T^k(LC_{-1}) = T^{k-1}(LC)$, LC_0 being LC.

A chaotic area $\mathscr{A}$ of the map T is an invariant set of T, i.e. $T(\mathscr{A}) \equiv \mathscr{A}$, which includes a chaotic set, and numerically computed trajectories seem to cover the area. Often its boundary can be obtained by following the procedure, described
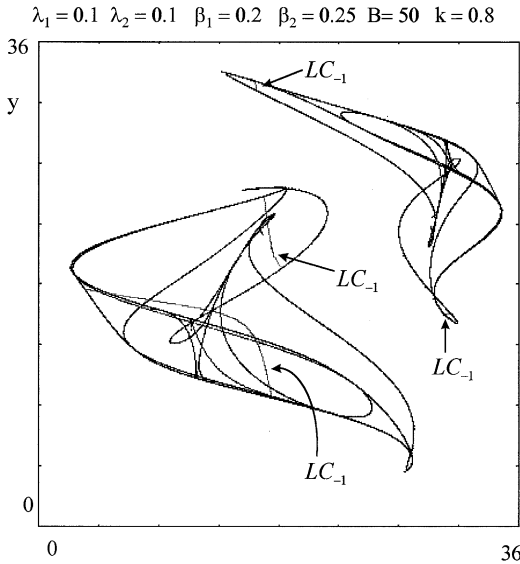
$\lambda_1 = 0.1$ $\lambda_2 = 0.1$ $\beta_1 = 0.2$ $\beta_2 = 0.25$ B= 50 k = 0.8

Fig. 6. Boundary of the attractor shown in Fig. 5b obtained by arcs of critical curves $LC, LC_1, \ldots, LC_6$, according to (23) with $m = 7$.

in Mira et al. (1996, Chapter 4). Let $\gamma = \mathscr{A} \cap LC_{-1}$ be the portion of critical curve of rank-0 inside $\mathscr{A}$. Then, for a suitable integer m

$$\partial\mathscr{A} \subseteq \bigcup_{k=1}^{m} T^k(\gamma). \tag{23}$$

An example is shown in Fig. 6, where the boundary of the 2-cyclic chaotic area of Fig. 5b is obtained by the images, up to rank 7, of the portion γ of LC_{-1}. In other words, the exact boundary of the chaotic attractor of Fig. 5b can be obtained by (23) with $m = 7$. It is worth noticing that the critical curves of increasing rank not only give the boundary of a chaotic attractor, but also the regions of greater density of points, i.e., the regions that are more frequently visited by the points of the generic trajectory in the invariant area $\mathscr{A}$.

The qualitative change that transforms the two-cyclic chaotic set shown in Fig. 5c into the 'one-piece' chaotic attractor of Fig. 5d can be described by a global bifurcation too. Such a bifurcation is characterized by a contact between critical curves and the stable manifold of the saddle fixed point E_*. We now show that this bifurcation is a homoclinic bifurcation, due to the creation of a transverse intersection between the stable and the unstable manifolds of the saddle fixed point E_* (for recent work on homoclinic bifurcations in economic models see, e.g., Gardini, 1993; de Vilder, 1996; Brock and Hommes, 1997). In

$\lambda_1 = 0.1$ $\lambda_2 = 0.102$ $\beta_1 = 0.2$ $\beta_2 = 0.2416$ B= 50 k = 0.8

(a)

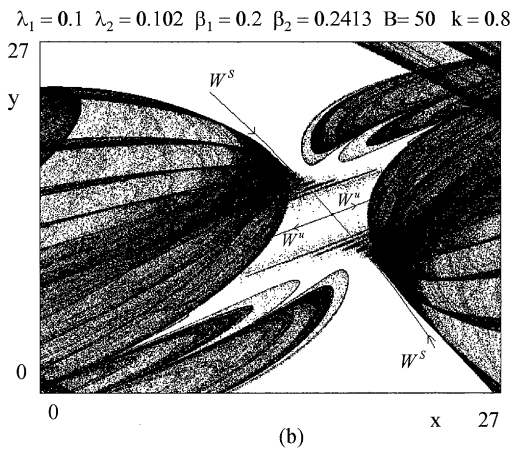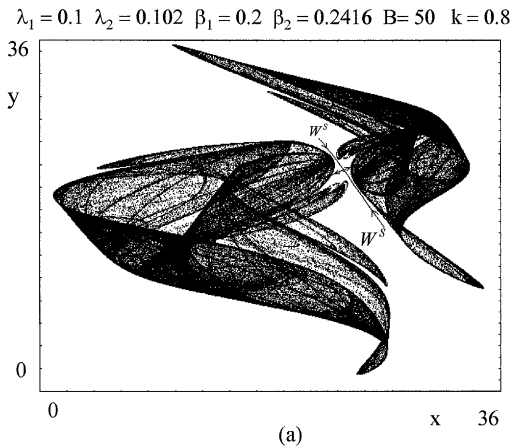$\lambda_1 = 0.1$ $\lambda_2 = 0.102$ $\beta_1 = 0.2$ $\beta_2 = 0.2413$ B= 50 k = 0.8

(b)

Fig. 7. Homoclinic bifurcation that marks the transformation of a 2-cyclic chaotic set into a one-piece chaotic set. W^u and W^s are the local unstable manifold and the local stable manifold of the saddle fixed point E_*, respectively. (a) Before the homoclinic tangency. (b) After the homoclinic tangency.

fact, decreasing β_2, starting from the value used in Fig. 5c, we see that the two portions of the 2-cyclic chaotic set approach each other, and are separated by the stable manifold $W^s(E_*)$ of the saddle point (see Fig. 7a). We recall that the two pieces of the cyclic chaotic area of T are two disjoint attractors for T^2, whose basins are separated by $W^s(E_*)$. This means that before the merging of the two pieces we have $W^s(E_*) \cap \mathscr{A} = \emptyset$. Moreover, the chaotic area $\mathscr{A}$ of T includes the closure of $W^u(E_*)$. We numerically see, by iterating a small

segment made up of points of $W^u(E_*)$, that the critical arcs of the boundary of $\mathscr{A}$ involved in the contact with $W^s(E_*)$, are made up of points of $W^u(E_*)$ or limit points of $W^u(E_*)$. At $\beta_2 = \beta_2^{(h)}$, the boundary $\partial\mathscr{A}$ has a contact with $W^s(E_*)$, which is, consequently, also a contact between $W^u(E_*)$ and $W^s(E_*)$. It is clear that while no homoclinic orbit of E_* exists for $\beta_2 > \beta_2^{(h)}$ (because $W^u(E_*)$ and $W^s(E_*)$ are disjoint) after the transversal crossing between $\partial\mathscr{A}$ and $W^s(E_*)$, occurring for $\beta_2 < \beta_2^{(h)}$, we have infinitely many intersections between $W^u(E_*)$ and $W^s(E_*)$. This clearly appears in the enlargement shown in Fig. 7b.

5. Conclusions

In this paper we investigated the global properties of a market share attraction model of interbrand competition by the method of critical curves. In contrast to existing studies of economic models, which primarily focus on the local dynamics and demonstrate the possibility of cyclic and erratic fluctuations by means of computer simulation, our work gives a fairly general investigation of the global dynamical behavior by a study of the properties of the attractors and of their basins. For the model analyzed in this paper the main qualitative changes of the global structure of the basins can be obtained by using the concept of critical curves. This allows us to learn more about the dynamical behavior of the system under study than by just focusing on local dynamics, since we obtain useful information on the size of the chaotic attractors and the structure of their basins of attraction. Both of the sequences of bifurcations described in this paper, either a change in the structure of $\mathscr{B}$ or a change in the structure of the attracting set caused by increasing one or both of the speeds of adjustment λ_i, result in a loss of predictability of the asymptotic behavior of the economic system. On the one hand, the global bifurcations of the boundaries of $\mathscr{B}$ cause an increasing uncertainty with respect to the destiny of an economic system starting from a given initial state. A small change in the initial condition, i.e., a small change in initial marketing efforts, or a small exogenous shock during the adjustment process, may cause a great modification of the long-run behavior of the system, since it can be transformed from a bounded process into a non-feasible one. On the other hand, the local and global bifurcations that change the structure of the attractor $\mathscr{A}$ give rise to an increasing loss of information about the asymptotic evolution of the system. The convergence to the well-known steady state is replaced — for increasing values of the speeds of adjustment — by an asymptotic convergence to a periodic cycle, with predictable cyclic values of the state variables, and then by a cyclic behavior with output levels which are not well predictable since they fall inside cyclic chaotic areas. Finally, a situation of erratic behavior inside a large area of the strategy space with no apparent periodicity may occur.

For the marketing theorist these results may be interesting, since the delimitation of the basin of attraction of a locally stable set permits one to understand if a given exogenous shock can be recovered by the endogenous dynamics of the economic system, or if it will cause an irreversible departure from the attractor. In terms of marketing theory our analysis might offer an explanation for the existence of various types of marketing institutions as some kind of 'disequilibrium mechanisms' designed to buffer or reduce the effects of complex dynamics (see Hibbert and Wilkinson, 1994). In any event, this type of analysis reveals which values of the parameters lead to erratic, random-looking patterns often found in marketing time series (see Bishop et al., 1984; Priesmeyer, 1992). Our analysis also shows that the parameters λ_1 and λ_2, which are under the decision makers' control, are critical in the sense that their values determine the dynamics of the system.

Although economists mainly focused on one-dimensional systems, more recent publications indicate an increasing interest in higher-dimensional economic models (see Gardini, 1992, 1993; Delli Gatti et al., 1993; Hommes, 1998; Gardini, 1994; de Vilder, 1996; Brock and Hommes, 1997; for the study of homoclinic bifurcations). Consequently, it seems that mathematical methods developed to study higher-dimensional (particularly, two-dimensional) systems will play a considerable role in economics.

References

Abraham, R., Gardini, L., Mira, C., 1997. Chaos in Discrete Dynamical Systems, A Visual Introduction in Two Dimension. Springer, Berlin.

Bell, D.E., Keeney, R.L., Little, J.D.C., 1975. A market share theorem. Journal of Marketing Research 12, 136–141.

Bischi, G.I., Stefanini, L., Gardini, L., 1998. Synchronization, intermittency and critical curves in a duopoly game. Mathematics and Computers in Simulation 44, 559–585.

Bishop, W.S., Graham, J.L., Jones, M.H., 1984. Volatility of derived demand in industrial markets and its management implications. Journal of Marketing 48, 95–103.

Brock, W.A., Hommes, C.H., 1997. A rational route to randomness. Econometrica 65, 1059–1095.

Bultez, A.V., Naert, P.A., 1975. Consistent sum-constrained models. Journal of the American Statistical Association 70, 529–535.

Carpenter, G.S., Cooper, L.G., Hanssens, D.M., Midgley, D.F., 1988. Modeling asymmetric competition. Marketing Science 7, 393–412.

Cooper, L., 1988. Competitive maps: The structure underlying asymmetric cross elasticities. Management Science 34, 707–723.

Cooper, L.G., Nakanishi, M., 1988. Market-Share Analysis. Kluwer Academic Publishers, Dordrecht.

Cowling, K., Cubbin, J., 1971. Price, quality and advertising competition: an econometric investigation of the United Kingdom car market. Economica, 378–394.

Day, R.H., 1994. Complex Economic Dynamics. vol. I: An Introduction to dynamical Systems and Market Mechanisms. MIT Press, Cambridge, MA.

Delli Gatti, D., Gallegati, M., Gardini, L., 1993. Investment confidence, corporate debt and income fluctuations. Journal of Economic Behavior and Organization 22, 161–187.

Devaney, R.L., 1989. An Introduction to Chaotic Dynamical Systems. The Benjamin/Cummings Publishing Co., Menlo Park.

Feichtinger, G., Hommes, C.H., Milik, A., 1994. Complex dynamics in a threshold advertising model. OR Spektrum 16, 101–111.

Feinberg, F.M., 1992. Pulsing Policies for aggregate advertising models. Marketing Science 11, 221–234.

Gardini, L., 1992. Some global bifurcations in two-dimensional endomorphisms by use of critical curves. Nonlinear Analysis, TMA 18, 361–399.

Gardini, L., 1993. On a model of financial crisis: critical curves as new tools of global analysis. in: Gori, F., Galeotti, M. (Eds.), Nonlinear Dynamics in Economics and Social Sciences. Springer, Berlin, pp. 252–263.

Gardini, L., 1994. Homoclinic bifurcations in n-dimensional endomorphisms, due to expanding periodic points. Nonlinear Analysis, TMA 23, 1039–1089.

Guckenheimer, J., Holmes, P., 1983. Nonlinear Oscillations, Dynamical Systems, and Bifurcations of Vector Fields. Springer, Berlin.

Gumowski, I., Mira, C., 1980. Dynamique Chaotique, Cepadues Editions, Toulose.

Hibbert, B., Wilkinson, I.F., 1994. Chaos theory and the dynamics of marketing systems. Journal of the Academy of Marketing Science 22, 218–233.

Hommes, C., 1991. Chaotic Dynamics in Economic Models. Some Simple Case-Studies. Wolters-Noordhoff, Groningen.

Hommes, C.H., 1998. On the consistency of backward looking expectations: The case of the cobweb. Journal of Economic Behavior and Organization 33, 333–362.

Kopel, M., 1996a. Periodic and chaotic behavior of a simple R&D model. Ricerche Economiche 50, 235–265.

Kopel, M., 1996b. Simple and complex adjustment dynamics in Cournot Duopoly models. Chaos, Solitons, and Fractals 7, 2031–2048.

Kopel, M., Dawid, H., Feichtinger, G., 1998. Periodic and chaotic programs of intertemporal optimization models with nonconcave net benefit function. Journal of Economic Behavior and Organization 33, 435–447.

Luhta, I., Virtanen, I., 1996. Non-linear advertising capital model with time delayed feedback advertising and stock of goodwill. Chaos, Solitons and Fractals 7, 2083–2104.

Mahajan, V., Muller, E., 1986. Advertising pulsing policies for generating awareness for new products. Marketing Science 5, 89–106.

Milnor, J., 1985. On the concept of attractor. Communications in Mathematical Physics 99, 177–195.

Mira, C., 1987. Chaotic Dynamics. World Scientific, Singapore.

Mira, C., Fournier-Prunaret, D., Gardini, L., Kawakami, H., Cathala, J.C., 1994. Basin bifurcations of two-dimensional noninvertible maps: fractalization of basins. International Journal of Bifurcations and Chaos 4, 343–381.

Mira, C., Gardini, L., Barugola A., Cathala, J.C., 1996. Chaotic Dynamics in Two-Dimensional Noninvertible Maps. World Scientific, Singapore.

Park, S., Hahn, M., 1991. Pulsing in a discrete model of advertising competition. Journal of Marketing Research 28, 397–405.

Parker, D., Stacey, R., 1994. Chaos, management and economics: the implications of nonlinear thinking. Hobarth paper 125, The Institute of Economic Affairs.

Priesmeyer, R.H., 1992. Organizations and Chaos. Defining the Methods of Nonlinear Management. Quorum Books.

Rossiter, J.R., Percy, L., 1987. Adverstising and Promotion Management. McGraw-Hill, New York.

Simon, H., 1982. ADPULS: an advertising model with wearout and pulsation. Journal of Marketing Research 19, 352–363.

Sterman, J.D., 1989a. Modeling managerial behavior: misperceptions of feedback in a dynamic decision making experiment. Management Science 35, 321–339.

Sterman, J.D., 1989b. Deterministic chaos in an experimental economic system. Journal of Economic Behavior and Organization 12, 1–28.

Thietart, R.A., Forgues, B., 1995. Chaos theory and the organization. Organization Science 6, 19–31.

Tversky, A., Kahneman, D., 1975. Judgement und uncertainty: heuristics and biases. Science 185, 1124–1131.

de Vilder, R., 1996. Complicated endogenous business cycles under gross substitutability. Journal of Economic Theory 71, 416–442.